Kidney Diseases

Research Article

Kidney Dis 2023;9:58–71
DOI: 10.1159/000528010

Received: March 12, 2022
Accepted: October 26, 2022
Published online: November 29, 2022

Loss of Pten in Renal Tubular Cells Leads to Water Retention by Upregulating AQP2

Zhuo Sun[a] Xiaotong Shao[a] Haotian Wu[a] Yaxian Zhao[b] Yidan Cao[c] Danhua Li[a] Ying Sun[d] Qingling Wang[a]

[a]Department of Pathology, Laboratory of Clinical and Experimental Pathology, Xuzhou Medical University, Xuzhou, China; [b]Department of Pathology, Xuzhou Maternity and Child Health Care Hospital, Xuzhou, China; [c]Department of Pathology, Wuxi No.2 People's Hospital, Wuxi, China; [d]Jiangsu Key Laboratory of New Drug Research and Clinical Pharmacy, Xuzhou Medical University, Xuzhou, China

Keywords
PTEN · Kidney · AQP2 · Water retention

Abstract
Introduction: Phosphatase and tensin (PTEN) is a multifunctional gene associated with the normal development and physiological function of various tissues including the kidney. However, its role in renal tubular reabsorption function has not been well elucidated. ***Methods:*** We generated a renal tubule-specific *Pten* knockout mouse model by crossing *Pten*$^{fl/fl}$ mice with *Ksp-Cre* transgenic mice, evaluated the effect of *Pten* loss on renal tubular function, and investigated the underlying mechanisms. ***Results:*** *Pten* loss resulted in abnormal renal structure and function and water retention in multiple organs. Our results also demonstrated that aquaporin-2 (AQP2), an important water channel protein, was upregulated and concentrated on the apical plasma membrane of collecting duct cells, which could be responsible for the impaired water balance in *Pten* loss mice. The regulation of *Pten* loss on AQP2 was mediated by protein kinase B (AKT) activation. ***Conclusions:*** Our results reveal a connection between *PTEN* gene inactivation and water retention, suggesting the importance of PTEN in normal kidney development and function.

Introduction

The kidney is the main organ for filtering blood and removing waste and excess water. The glomeruli filter fluids and small waste substances out of the blood, whereas the renal tubules reabsorb the needed substances including water back into the blood. Waste products and excess fluid are finally excreted as urine [1]. During this process, the collecting ducts are the main parts of the kidney and are responsible for water reabsorption. The collecting ducts reabsorb sodium and water from the primary urine and excrete potassium into the urine through the sodium-potassium channel and vasopressin-sensitive water channel aquaporin-2 (AQP2), respectively [2, 3].

AQP2 is a member of the aquaporin (AQP) family that plays a pivotal role in urine concentration and body water balance. Impaired AQP2 expression or localization led to various water balance disorders such as nephrogenic diabetes insipidus (NDI) [4], cirrhosis [5], severe congestive heart failure [6, 7], and syndrome of inappropriate antidiuretic hormone secretion (SIADH) [8]. AQP2 is mainly expressed in collecting duct principal cells, where it is usually localized in Rab11-positive intracellular vesicles in the basal state. In the presence of external stimuli, AQP2 is transported to the apical cell membrane and forms water channels to facilitate water influx [9, 10].

Karger@karger.com
www.karger.com/kdd

Correspondence to:
Qingling Wang, qlwang@xzhmu.edu.cn

AQP2 translocation could be regulated by posttranslational modifications. Among them, the phosphorylation of serine 256 residue is necessary for membrane accumulation of AQP2 [11–14]. Several protein kinases have been proved to be involved in this process, such as protein kinase A (PKA) [15–17], protein kinase G (PKG) [18], Golgi apparatus casein kinase (G-CK) [19], Ca^{2+}/calmodulin-dependent protein kinase II (CAMK2), protein kinase C-δ (PKCδ), and protein kinase B (AKT) [20].

Phosphatase and tensin (PTEN) homolog gene deleted on chromosome 10 is a dual-specificity phosphatase that can negatively regulate AKT activation by blocking its phosphorylation [21]. PTEN is generally expressed in all renal structures, especially in renal tubular cells [22]. PTEN loss or mutation is associated with various kidney diseases, such as clear cell renal cell carcinoma [23], acute kidney injury [24], renal fibrosis [25], and diabetic kidney disease [26]. However, the effect of PTEN loss on renal tubular reabsorption has not been well elucidated.

Based on previous studies, we speculate that PTEN may regulate AQP2 by AKT dephosphorylation and participate in maintaining water balance. To verify this, we established a kidney-specific *Pten* knockout mouse model and found that *Pten* loss resulted in abnormal renal structure and function and water retention. We demonstrated that AKT hyperactivation caused by PTEN loss upregulated AQP2 phosphorylation and enhanced water reabsorption in the kidney. Our data revealed the novel function of PTEN in regulating water balance and provided valuable targets for therapeutic intervention of water balance disorders.

Materials and Methods

Mice Breeding

Pten$^{\Delta/\Delta}$ mice (*Pten*$^{fl/fl}$; *Ksp-cre*) were generated by crossing *Pten*$^{fl/fl}$ mice (C57BL/6J background, Jackson laboratory) and *Ksp-Cre* mice (C57BL/6J background, the State Key Laboratory of Natural and Biomimetic Drugs, Peking University). Controls were *Pten*$^{fl/fl}$ littermates without *Ksp-Cre* expression. All animals were fed with standard diet and drinking water freely and were kept under fixed ambient conditions (23 ± 1°C, 12/12 h light/dark cycle).

Genotyping

Genomic DNA was extracted from the mouse tail for polymerase chain reaction (PCR) genotyping analysis. TransGen PCR SuperMix (AS111-11, TransGen) was used for PCR following the manufacturer's protocol. PCR primers used for genotyping were *Pten*-F: 5′-CAAGCACTCTGCGAACTGAG-3′; *Pten*-R: 5′-AAGTTTTTGAAGGCAAGATGC-3′ to detect *Pten*-floxed allele; *Ksp-cre*-F: 5′-GCAGATCTGGCTCTCCAAAG-3′; *Ksp-cre*-R: 5′-AGGCAAATTTTGGTGTACGG-3′ to detect *Ksp-Cre* allele.

Brain Water Content Determination

After mice were euthanized, brains were removed and weighed immediately (wet weight). Then, brains were dried in a desiccation oven for 48 h at 80°C and weighed again (dry weight). Brain water content (%) was calculated as follows: (wet weight-dry weight)/wet weight × 100%.

Immunohistochemistry

Tissues harvested from mice were fixed in formalin solution and embedded in paraffin. Tissues were then cut into 5 μm slices and incubated with primary antibodies after antigen retrieval. Anti-mouse/rabbit immunohistochemistry detection kit (PK10006, Proteintech) was used for color development. After counterstained with hematoxylin, slides were mounted with neutral gum and evaluated under a microscope. The primary antibodies included anti-PTEN (9188L, CST, 1:150) and anti-AQP2 (AQP-002, Alomone, 1:200).

Immunofluorescence

Tissues were embedded with optimum cutting temperature compound (4583, Sakura) and cut into 5 μm slices. The slides were fixed in 4% paraformaldehyde for 10 min and blocked with 10% goat serum. After incubation with primary antibody at 4°C overnight, fluorescent secondary antibody (Alexa Fluor 488, Invitrogen, 1:500) was used for 2 h at room temperature. Then, the cryosections were mounted with DAPI-containing medium (KGA215-10, KeyGen) and observed under a fluorescence microscope. The primary antibody included anti-AQP2 (AQP-002, Alomone, 1:200).

Cell Culture

The mouse inner-medullary collecting duct (IMCD3) cells were obtained from Shanghai Jihe Biotechnology and cultured in DMEM/F12 medium containing 10% fetal bovine serum at 37°C in a humidified incubator with 5% CO_2. After reaching 80% confluency, cells were treated with 20 mM LY294002 (GC15485, GlpBio) for 24 h and then subjected to immunoblot analysis.

Short Hairpin RNA Transfection

The cells were plated into 24-well plates 1 day before transfection. 25 μL short hairpin RNA (shRNA)-containing lentivirus was then added to medium with 5 μg/mL polybrene. After 24 h incubation, virus-containing medium was removed, and cells were cultured for another 48 h before they were finally collected for subsequent experiments. PTEN-targeted shRNA (5′-GACAAAGCCAACCGATACTTT-3′) and control shRNA (5′-TTCTCCGAACGTGTCACGT-3′) were obtained from GenePharma.

Western Blotting

Tissues and cells were lysed in RIPA buffer for total protein. Membrane protein was obtained by membrane and cytosol protein extraction kit (P0033, Beyotime) according to manufacturer's procedures. Proteins were separated by sodium dodecyl sulfate-polyacrylamide gel electrophoresis on 8–10% gel and then transferred to polyvinylidene fluoride membrane. After blocked in 5% skim milk, the membranes were incubated with primary antibodies: anti-PTEN (9188L, CST, 1:2,000), anti-AQP2 (AQP-002, Alomone, 1:2,000), anti-pSer256-AQP2 (bs-12507R, Bioss, 1:500), anti-AKT (4691S, CST, 1:2,000), anti-pSer473-AKT (4060S, CST,

1:2,000), and anti-GAPDH (60004-1-Ig, Proteintech, 1:5,000) at 4°C overnight. HRP-conjugated secondary antibodies were incubated at room temperature for 2 h. Finally, proteins were visualized by enhanced chemiluminescence detection kit (E412, Vazyme).

Real-Time PCR Analysis

RNA was extracted using total RNA extraction reagent (R401-01, Vazyme) and reverse transcribed to cDNA using HiScript Q RT SuperMix (R222-01, Vazyme). According to manufacturer's specifications, Cham Q SYBR qPCR Master Mix (Q331-02, Vazyme) was used to perform three replicates of PCR in a 10 μL reaction volume. The mRNA expression of target genes was normalized to GAPDH and calculated using a comparative CT ($2^{-\Delta\Delta Ct}$) method. The primers were AQP2-F: 5′-GGACCTGGCTGTCAATGCTC-3′ and AQP2-R: 5′-GCGGGCTGGATTCATGGAG-3′.

Renal Function Measurement

Mouse serum was collected by centrifugation after blood collection from suborbital vein and was determined by Creatinine Assay Kit (C011-2-1, Nanjing Jiancheng). Urine samples were collected by the metabolic cage for 24 h and then determined by Urea Assay Kit (C013-2-1, Nanjing Jiancheng). The urine sample osmotic pressure was measured by freezing point osmometer (OM806, Loser).

Statistical Analysis

The significance between two groups was analyzed using Student's *t* test and statistical comparisons among multiple groups were analyzed using analysis of variance followed by Student-Newman-Keul's test for pairwise comparisons. All analyses were performed in SPSS 16.0. $p < 0.05$ was considered statistically significant.

Results

Construction and Identification of Renal Tubule-Specific Pten Knockout Mice

To investigate the physiological effect of PTEN on renal tubules, we generated a renal tubule-specific *Pten* knockout mouse model (herein, $Pten^{\Delta/\Delta}$ mice) by crossing $Pten^{fl/fl}$ mice with *Ksp-Cre* transgenic mice in which Cre recombinase was driven by the kidney-specific cadherin promoter and mainly expressed in distal tubules, ascending and descending loops of Henle, and collecting ducts [27] (shown in Fig. 1a). *Pten* deletion and *Ksp-Cre* expression in the kidneys of the $Pten^{\Delta/\Delta}$ mice were verified by PCR analysis. PCR of the genomic DNA detected Cre recombinase only in $Pten^{\Delta/\Delta}$ mice but not in the wild-type littermate control ($Pten^{fl/fl}$) mice (shown in Fig. 1b), confirming that $Pten^{\Delta/\Delta}$ mice underwent Ksp-Cre-mediated recombination successfully. Western blot analysis of the whole kidney lysate also revealed a significant decrease in PTEN levels in $Pten^{\Delta/\Delta}$ mice (shown in Fig. 1c). We further examined the expression of PTEN protein in the kidney by immunohistochemistry (IHC) staining and found that PTEN was normally expressed in control mice but was absent in distal tubules and collecting ducts of $Pten^{\Delta/\Delta}$ mice (shown in Fig. 1d).

Renal Tubule-Specific Deletion of Pten Led to Abnormal Kidney Structure and Function

Cohorts of $Pten^{\Delta/\Delta}$ mice aged 10–12 months ($n = 32$) were analyzed. The external appearance and weight of these $Pten^{\Delta/\Delta}$ mice were indistinguishable from those of control mice (shown in Fig. 2a). However, their kidneys were of different size and weight (shown in Fig. 2b), and $Pten^{\Delta/\Delta}$ mice had enlarged and heavier kidneys than control mice. Results of the histological analysis showed remarkable expansion of distal tubules and collecting ducts in $Pten^{\Delta/\Delta}$ mice (shown in Fig. 2c) in the cortex and medulla. Moreover, histologic lesions included cell swelling and exfoliation of epithelial cells could be found (shown in online suppl. Fig. S1a; for all online suppl. material, see www.karger.com/doi/10.1159/000528010).

Some (8 of 32) of the $Pten^{\Delta/\Delta}$ mice displayed hydronephrosis, which occurred in both females and males (shown in Fig. 2d). Urinary flow obstruction was a common contributing factor to hydronephrosis [28]. $Pten^{\Delta/\Delta}$ mice showed remarkable hyperproliferation of the urothelium (shown in online suppl. Fig. S1b). However, they did not exhibit ureteral obstruction or stricture, suggesting that urinary flow obstruction does not cause hydronephrosis.

Moreover, two $Pten^{\Delta/\Delta}$ mice had renal tumors (shown in online suppl. Fig. S1c). The tumor compressed the surrounding tissue and caused extensive renal fibrosis. Under microscope observation, the tumor was composed of large cystic cells with significant atypia, pathologic mitotic figure, and infiltration of surrounding tissues (shown in online suppl. Fig. S1d).

Fig. 1. Construction and identification of renal tubules-specific *Pten* knockout mice. **a** *Ksp-Cre* mice were crossed with $Pten^{fl/fl}$ mice to generate $Pten^{\Delta/\Delta}$ mice. **b** Tail DNA extracted from different mice were analyzed by PCR to determine the genotypes. The positions of the bands representing floxed *Pten* (328bp), wild-type *Pten* (156bp), and *Ksp-Cre* (420bp) alleles were indicated. **c** PTEN was decreased in the kidney of $Pten^{\Delta/\Delta}$ mice versus $Pten^{fl/fl}$ (control) mice as assessed by Western blotting (***$p \leq 0.001$). **d** PTEN IHC images corresponding to kidney cortex and medulla from mice. pt, proximal tubule; dt, distal tubule; cd, collecting duct. Bars = 100 μm.

(For figure see next page.)

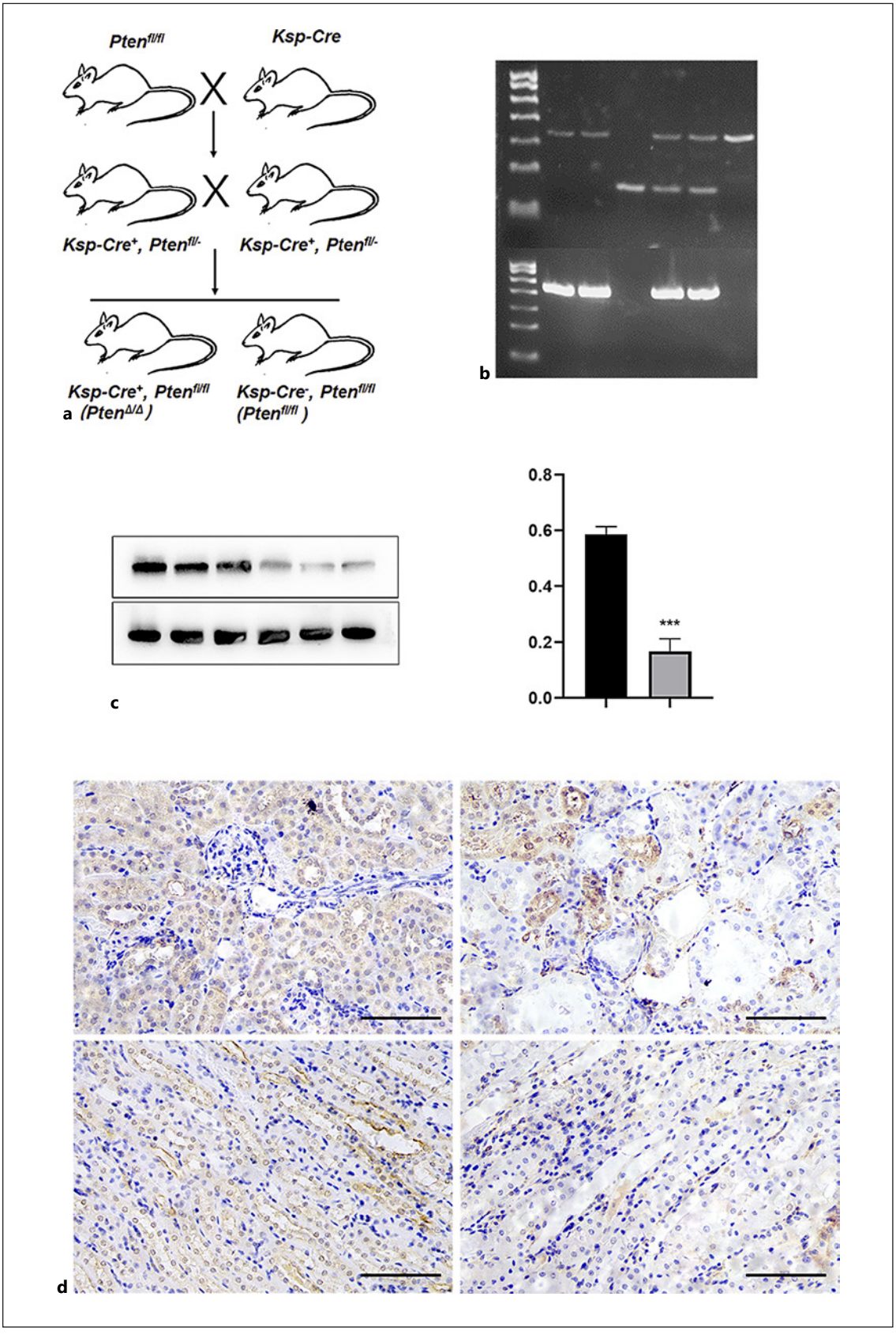
Pten^fl/fl
Ksp-Cre
Ksp-Cre+, Pten fl/-
Ksp-Cre+, Pten fl/-
Ksp-Cre+, Pten fl/fl
(Pten Δ/Δ)
Ksp-Cre-, Pten fl/fl
(Pten fl/fl)
a
b
c
0.8
0.6
0.4
0.2
0.0
***
d

1

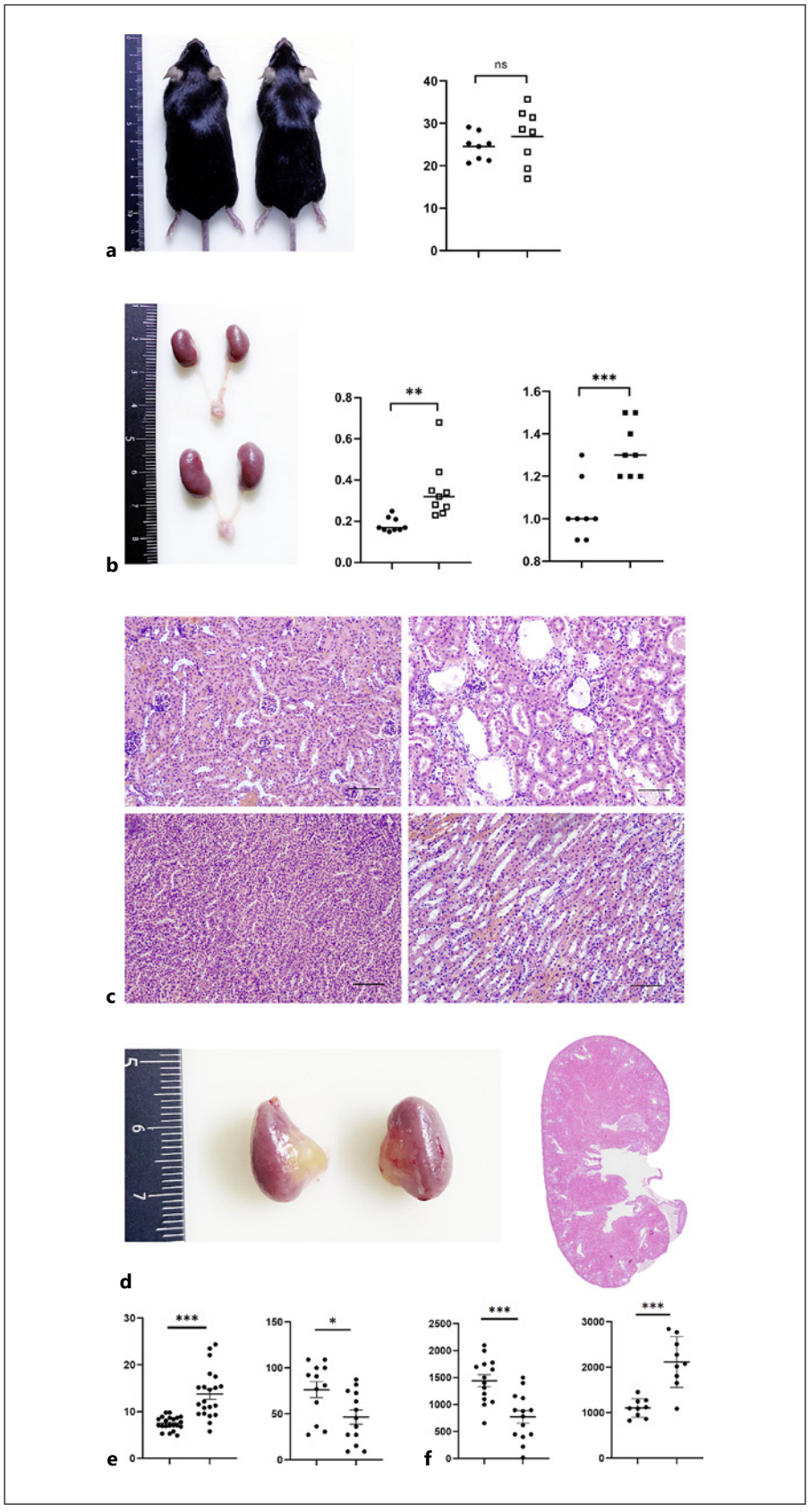

Fig. 2. Renal tubules-specific deletion of *Pten* led to abnormal kidney structure and function. **a** Macroscopic characteristics of $Pten^{fl/fl}$ and $Pten^{\Delta/\Delta}$ mice. **b** Kidneys from $Pten^{\Delta/\Delta}$ mice were significantly bigger, and no apparent blockage of the ureter was detected. Kidney weight and length were measured in each group. **c** Comparison of histopathology of renal cortex and medulla from $Pten^{fl/fl}$ and $Pten^{\Delta/\Delta}$ mice. Bars = 100 μm. **d** Example of hydronephrosis in $Pten^{\Delta/\Delta}$ mice. **e** Analysis of BUN and SCr in $Pten^{fl/fl}$ and $Pten^{\Delta/\Delta}$ mice. **f** Quantitative plots showed less urine excretion and increased urine osmolality of $Pten^{\Delta/\Delta}$ mice in comparison with $Pten^{fl/fl}$ mice ($n \geq 8$ per genotype). $^{*}p < 0.05$, $^{**}p < 0.02$, $^{***}p < 0.001$.

The aforementioned lesions in *Pten*$^{\Delta/\Delta}$ mice indicated that they might suffer renal insufficiency at this stage. To evaluate the influence of *Pten* knockout on renal function, we detected renal function indexes including blood urea nitrogen and serum creatinine in both groups. As shown in Figure 2e, blood urea nitrogen levels in *Pten*$^{\Delta/\Delta}$ mice were markedly higher, whereas serum creatinine levels were lower than those of the control mice, suggesting renal function insufficiency in *Pten*$^{\Delta/\Delta}$ mice. Furthermore, *Pten*$^{\Delta/\Delta}$ mice had a decreased 24 h urine volume but increased urine osmolality (shown in Fig. 2f), indicating an enhanced urine concentration function.

Pten Knockout in the Kidney Caused Water Retention in Various Organs

Histopathological assessment of other organs was also performed. The liver of *Pten*$^{\Delta/\Delta}$ mice had increased weight and was apparently lighter in color (shown in Fig. 3a). Hepatocytes were severely enlarged, and the cytoplasm was swelling and even vacuolated (shown in Fig. 3b). The brain of *Pten*$^{\Delta/\Delta}$ mice was also pale and slightly enlarged with swollen olfactory bulb. The brain water content of *Pten*$^{\Delta/\Delta}$ mice was higher than that of control mice (shown in Fig. 3c), suggesting cerebral edema. Moreover, the size and weight of the heart of *Pten*$^{\Delta/\Delta}$ mice increased, with pronounced thickening of the left ventricular wall (shown in Fig. 3d), indicating an increase in blood volume. Together, these data revealed that *Pten* knockout in the kidney led to water retention in multiple organs and suggested impaired regulation of the body water balance in *Pten*$^{\Delta/\Delta}$ mice.

AQP2 Was Upregulated and Concentrated in the Apical Plasma Membrane of Collecting Duct Cells in the Kidneys of Pten$^{\Delta/\Delta}$ *Mice*

AQPs are a family of small transmembrane proteins that play a pivotal role in maintaining water balance. Thirteen species of AQPs have been found in mammals (AQP0-AQP12) [29, 30], among which AQP2 is a key regulator of body water homeostasis and is expressed in medullary collecting ducts [31]. Therefore, to determine whether the impaired water balance correlated with AQP2, we evaluated *Aqp2* expression in the kidneys of *Pten*$^{\Delta/\Delta}$ mice by real-time PCR assay. As shown in Figure 4a, the expression of *Aqp2* mRNA was significantly increased in *Pten*$^{\Delta/\Delta}$ mice. Western blot analysis also demonstrated that both total AQP2 and phosphorylated AQP2 (pS256-AQP2) were upregulated in *Pten*$^{\Delta/\Delta}$ kidneys. The ratio of p-AQP2 to AQP2 increased in *Pten*$^{\Delta/\Delta}$ mice (shown in Fig. 4b).

IHC staining further showed that AQP2 was positively expressed in collecting ducts, and the staining intensity in *Pten*$^{\Delta/\Delta}$ mice was much higher than that in control mice (shown in Fig. 4c). Moreover, AQP2 expression was more concentrated on the apical plasma membrane of collecting duct cells in *Pten*$^{\Delta/\Delta}$ mice, whereas in *Pten*$^{fl/fl}$ mice, AQP2 was diffusely distributed in tubular cells (shown in Fig. 4d, e). All these results suggested that *Pten* knockout affected both the expression and distribution of AQP2, which could then enhance water reabsorption in the kidney and disrupt water balance.

PTEN Regulated AQP2 by Dephosphorylating p-AKT

To further investigate the underlying mechanism, we knocked down PTEN expression in IMCD3 cells and then detected AQP2 expression. As shown in Figure 5a, b, the mRNA and protein levels of AQP2 were significantly increased in PTEN knockdown IMCD3 cells (shPTEN), and p-AQP2 was also upregulated, which was consistent with our observation in *Pten*$^{\Delta/\Delta}$ mice.

Previous study [32] has reported the involvement of the PI3K/AKT pathway in regulating AQP2 expression and localization. Western blot analysis also showed upregulated AKT and phosphorylated AKT levels with an increased p-AKT/AKT ratio in the kidney medulla lysate of *Pten*$^{\Delta/\Delta}$ mice (shown in Fig. 5c), suggesting that AKT was activated after *Pten* deletion. Thus, we speculated that PTEN might regulate AQP2 by antagonizing the PI3K/AKT pathway. To verify this, LY294002 (LY), a PI3K inhibitor that acts on the ATP binding site of the catalytic subunit, was added to an IMCD3-shPTEN cell medium to suppress AKT activation. After 24 h of treatment, Western blot analysis showed that AKT phosphorylation was significantly blocked by LY and upregulated AQP2 and p-AQP2 in shPTEN cells were also reduced (shown in Fig. 5d). Moreover, increased membrane AQP2 and p-AQP2 in shPTEN cells were reversed by LY treatment (shown in Fig. 5e). MK-2206 (MK), another AKT specific inhibitor, showed effects similar to that of LY (shown in Fig. 5f, g). These results confirmed our speculation that AKT was an important mediator between PTEN and AQP2.

Conclusion

PTEN is a multifunctional gene associated with the normal development and physiological function of various tissues such as the liver, neurons, thyroid, lung, and kidney [33–40]. In this study, we investigated the

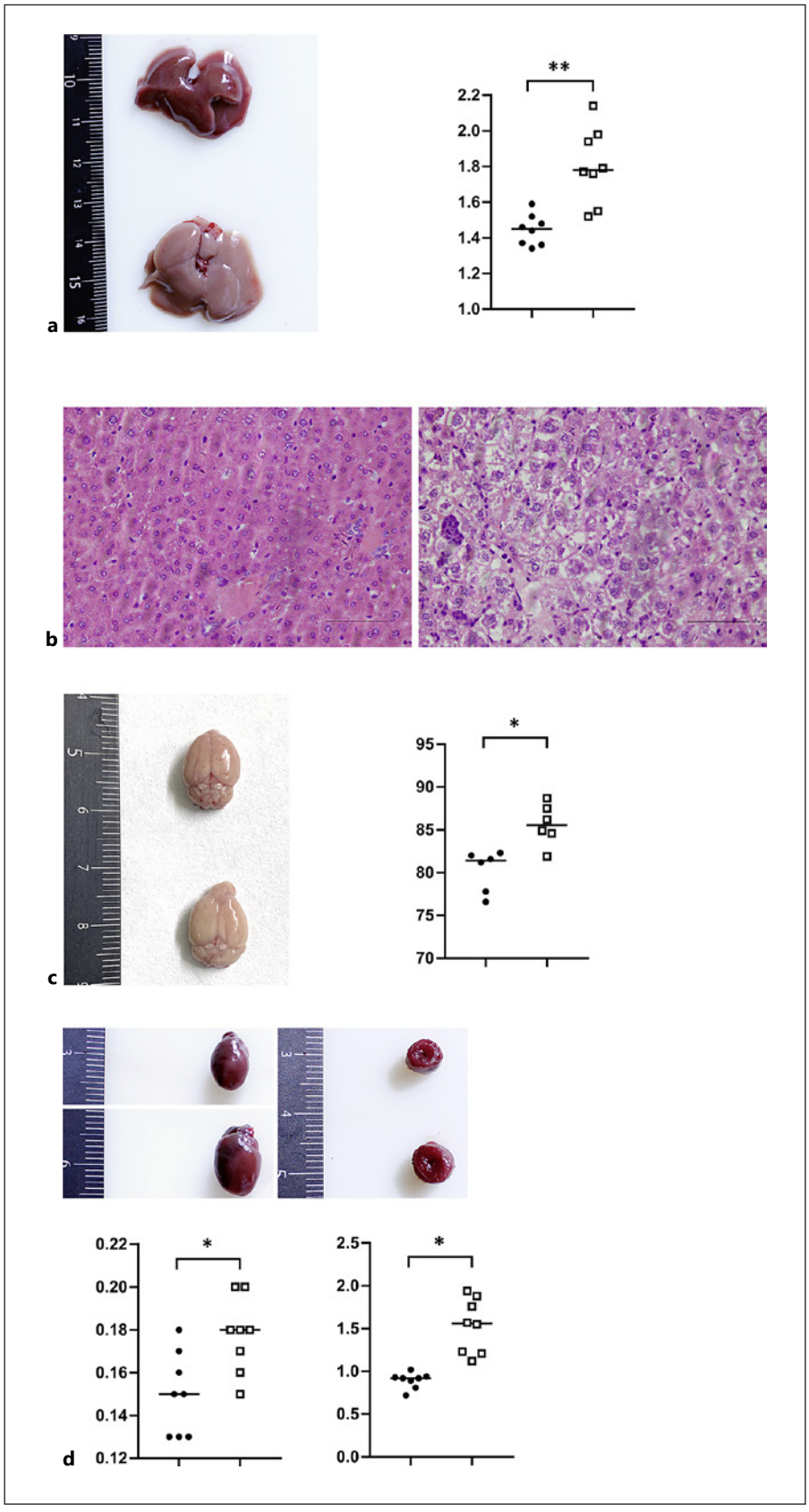

Fig. 3. *Pten* knockout in kidney caused water retention in multiple organs. **a** Gross appearance of liver and increased liver weight in $Pten^{\Delta/\Delta}$ mice (n = 8). **b** The cellular swelling of hepatocyte was severe in $Pten^{\Delta/\Delta}$ mice. Bars = 100 μm (**c**) Gross appearance of brain and higher brain water content in $Pten^{\Delta/\Delta}$ mice (n = 6). **d** Comparison of heart size and left ventricular wall between $Pten^{fl/fl}$ and $Pten^{\Delta/\Delta}$ mice (n = 8). *$p < 0.05$, **$p < 0.02$.

Kidney Dis 2023;9:58–71
DOI: 10.1159/000528010

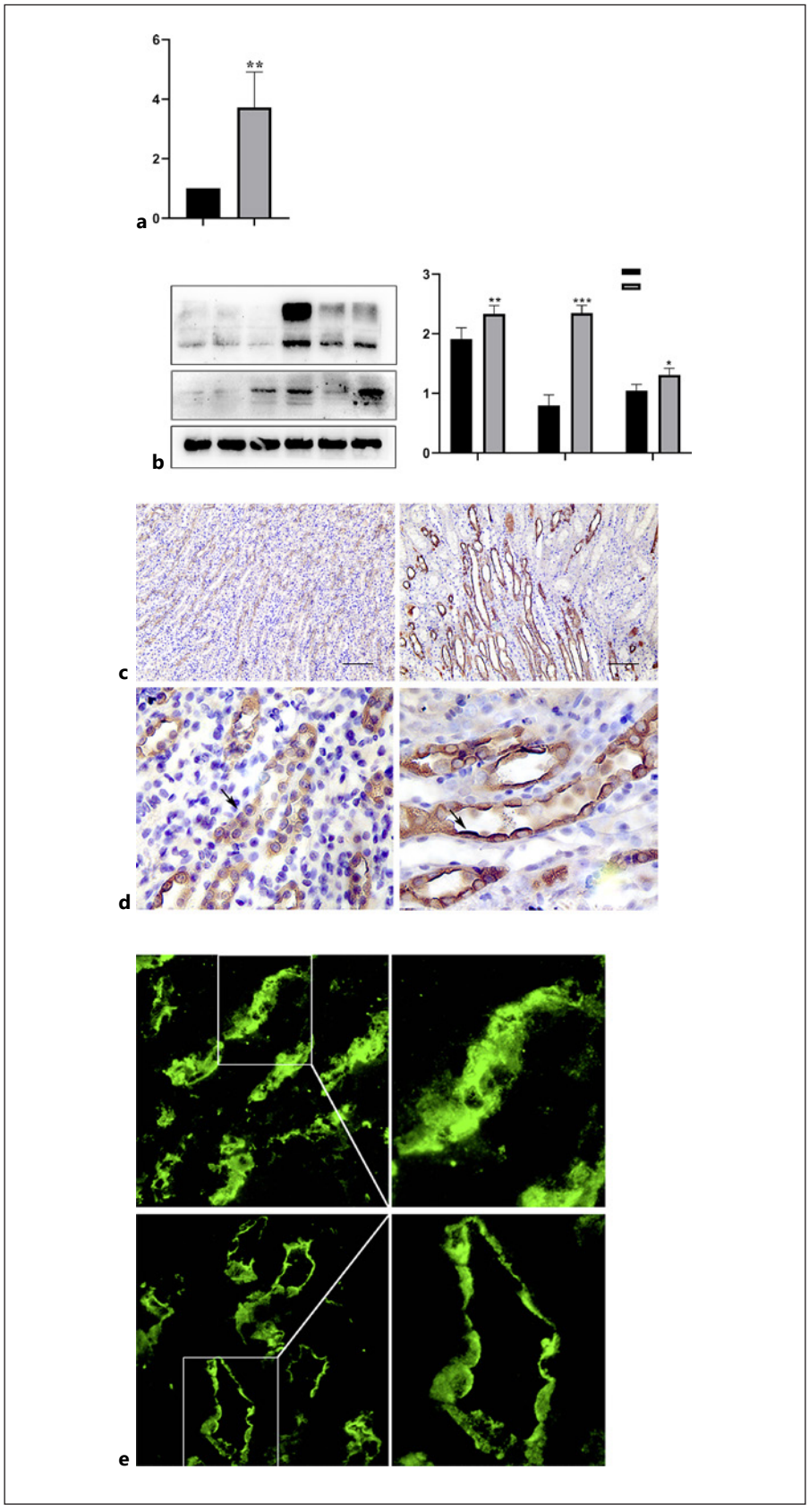

Fig. 4. AQP2 was upregulated and concentrated in the apical plasma membrane of collecting ducts cells in the kidney of $Pten^{\Delta/\Delta}$ mice. **a** The expression of *Aqp2* mRNA in the kidneys of $Pten^{fl/fl}$ and $Pten^{\Delta/\Delta}$ mice. **b** Western blots analysis of AQP2 and pS256-AQP2 levels in the kidney medulla lysates of $Pten^{fl/fl}$ and $Pten^{\Delta/\Delta}$ mice. **c** IHC staining of AQP2 in collecting ducts of $Pten^{fl/fl}$ and $Pten^{\Delta/\Delta}$ mice. Bars = 100 μm. **d** Higher magnification of IHC staining showed different distribution pattern of AQP2 in the collecting ducts cells of $Pten^{fl/fl}$ and $Pten^{\Delta/\Delta}$ mice. **e** Immunofluorescence staining of AQP2 (green) in collecting ducts of $Pten^{fl/fl}$ and $Pten^{\Delta/\Delta}$ mice. Higher magnifications of the selected areas are shown on the right.

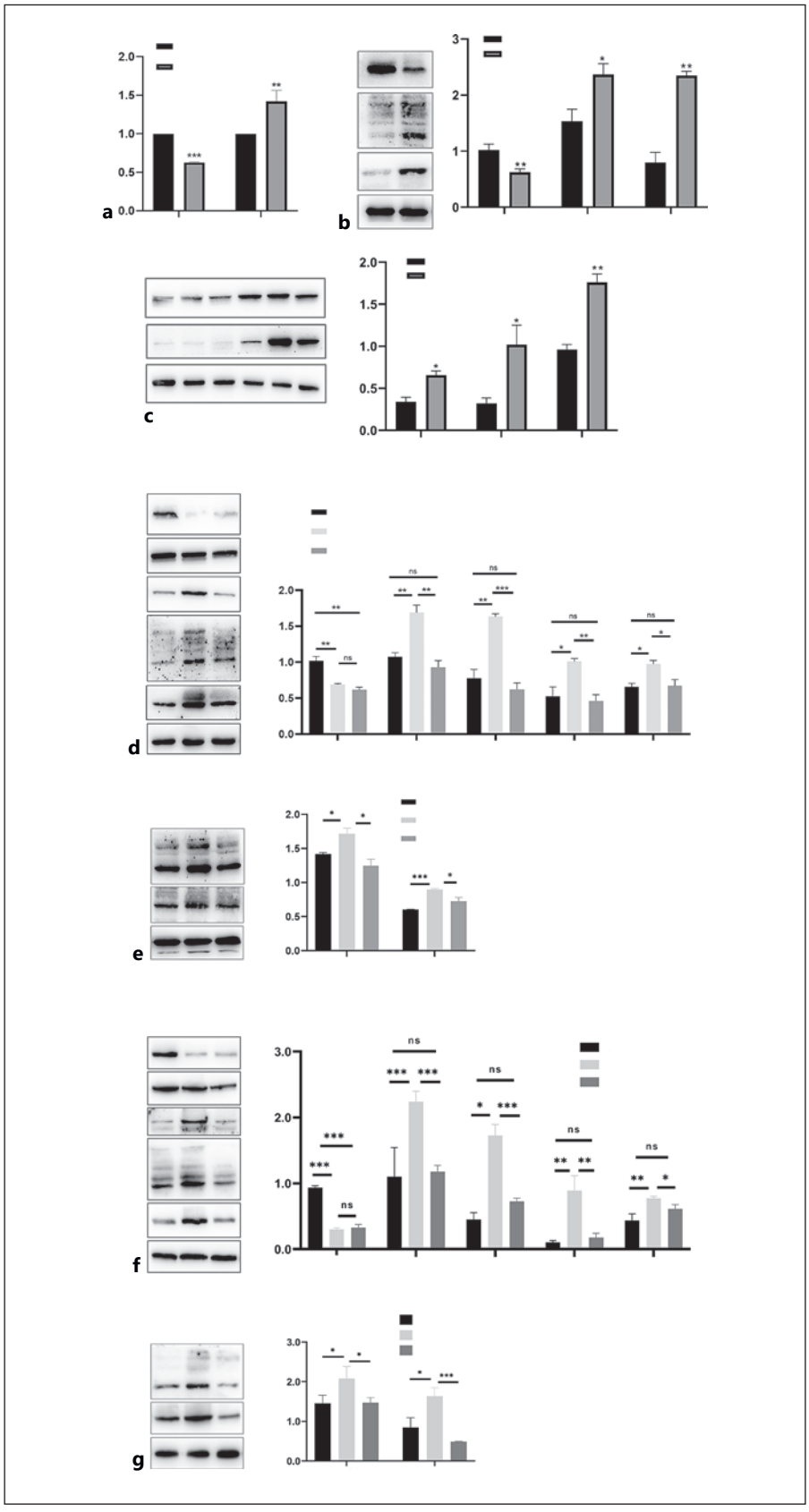

Fig. 5. PTEN regulated AQP2 by dephosphorylating p-AKT. **a** IMCD cells were transfected with control shRNA (shControl) or *Pten*-specific shRNA (shPTEN), respectively. Relative expression level of *Aqp2* genes in the shPTEN group is higher than that in the shControl group. **b** Western blots analysis of PTEN, AQP2, and p-AQP2 protein levels in shControl and shPTEN groups. **c** Western blots analysis of AKT and p-AKT proteins in kidney medulla lysates of $Pten^{fl/fl}$ and $Pten^{\Delta/\Delta}$ mice (n = 3 for each group). IMCD3-shPTEN cells were treated with LY (**d**) or MK (**f**) for 24 h and cell lysates of different groups were subjected to immunoblotting to detect the protein levels of AKT, p-AKT, AQP2, and p-AQP2 (n = 3-4 for each group). **e**, **g** Expression of membrane AQP2 (m-AQP2) and p-AQP2 (m-p-AQP2) in different groups of cells (n = 3 for each group). $^{ns}p > 0.05$, $^{*}p < 0.05$, $^{**}p < 0.02$, $^{***}p < 0.001$.

Kidney Dis 2023;9:58–71
DOI: 10.1159/000528010

function of PTEN in renal tubules by generating a renal tubule-specific *Pten* knockout mouse model ($Pten^{\Delta/\Delta}$). Renal structure and function were significantly impaired in $Pten^{\Delta/\Delta}$ mice. Water retention in multiple organs was also observed in $Pten^{\Delta/\Delta}$ mice, suggesting abnormal water reabsorption by renal tubules. Furthermore, AQP2, a water channel protein that is a key for water reabsorption, was upregulated in $Pten^{\Delta/\Delta}$ mice and concentrated on the apical plasma membrane of collecting ducts. To further explore the underlying mechanism of PTEN in regulating AQP2, we used a cell culture system of m-IMCD3, a mouse inner medulla-collecting duct cell line, and knockdown PTEN expression in IMCD3 cells (shPTEN). We found that PTEN knockdown activated AKT, which then phosphorylated AQP2 and facilitated its membrane translocation, whereas AKT inhibition could reverse these effects, suggesting that AKT activation is an important player in AQP2 regulation. Our study provides a connection between PTEN gene inactivation and water retention and indicates that PTEN can regulate water reabsorption function by AKT-mediated AQP2 phosphorylation and membrane concentration.

PTEN is widely expressed in all renal structures, including the glomeruli and renal tubules. Previous studies have reported that PTEN expressed in podocytes was associated with urinary albumin excretion and progression of diabetic kidney disease [41, 42]. However, the results were controversial for PTEN function in renal tubules. Zhou et al. [43] reported that *Pten* knockout in both proximal tubules and distal convoluted tubules had little effect on renal structure and function. However, in the study by Chen et al.[44], *Pten* loss in renal proximal tubules induced renal hypertrophy with markedly enlarged renal proximal tubules. Frew et al. [45] knocked out *Pten* in the distal convoluted tubules and collecting ducts and found that the kidney was almost normal, except for the development of urothelial hyperplasia in the renal pelvis and ureter, which was similar to the findings of Zhou. In the present study, we generated a mouse model with *Pten* deleted in the distal convoluted tubules and collecting ducts and found not only hyperproliferation of the urothelium but also the expansion of distal tubules and collecting ducts, hydronephrosis, and impaired renal function. These differences among the aforementioned mouse models might be attributed to the different Cre strains we used (Zhou used Nse-Cre, Chen used Ggt1-Cre, and Frew and our work used Ksp-Cre) and different mouse genetic backgrounds (C57BL/6J in Zhou's and our work and BALB/c background in Chen's and Frew's work). Although *Pten* loss alone was not sufficient to induce renal lesions in Zhou's and Frew's work, it could still markedly aggravate the lesions caused by the loss of other functional genes (such as *TSC1* and *pVHL*), which also suggested that PTEN helps in maintaining normal renal structure and function implicitly.

PTEN loss or mutation is frequently detected in RCC in humans [46, 47]. However, no renal tumors arose in the previous *Pten* knockout mouse model [41, 43–45], suggesting that *Pten* loss alone was insufficient to induce renal tumorigenesis. In this study, we first observed the renal tumors occurred in $Pten^{\Delta/\Delta}$ mice, although with a quite low probability (2 of 30). The tumors were both PAX8 (a specific marker for the kidney) positive and PTEN negative (data not shown), suggesting that they originated from the kidney and probably correlated with *Pten* loss. To confirm this, more renal tumor cases should be investigated, and further studies are needed in the future.

Hydronephrosis is the swelling of kidney caused by the buildup of water. A previous study has indicated that *Pten* loss in addition to pVHL ablation in the collecting ducts resulted in hydronephrosis [45], whereas in the present study, we observed that *Pten* loss alone was sufficient to cause hydronephrosis (although with a small probability, 8/30). Hydronephrosis is usually caused by urinary blockage or obstruction [48]. However, in our study, no severe obstruction was found in the renal pelvis and ureter of *Pten* knockout mice (shown in online suppl. Fig. S1b), which was similar to that observed by Frew [45]. In addition, we found increased AQP2 accompanied by decreased urine, which further led to water retention in the body. Thus, we thought that the hydronephrosis in the present study was not caused by urinary flow blockage but by impaired water balance.

Water homeostasis is critical for normal cell function and cellular processes, and the key event is water reabsorption mediated by water channel proteins in the renal collecting ducts. Water channel proteins, also called AQPs, are a family of small transmembrane proteins that play a pivotal role in transferring small molecules and water through biological membranes. Many AQPs are expressed in the kidney [29, 30], among which AQP2-4 are the major AQPs expressed in the medullary collecting ducts and related to water handling [49–51]. We detected the mRNA expressions of all three AQPs and found marked upregulation of AQP2, whereas slight downregulation of AQP3 and unaltered AQP4 in $Pten^{\Delta/\Delta}$ mice (data not shown), suggesting that PTEN loss has a more pronounced effect on AQP2 instead of AQP3 or AQP4. In addition, functional AQP2 is localized in the apical plasma

membrane of collecting duct primary cells to facilitate water influx [29, 49], which is the most critical process for water reabsorption in the kidney. Considering these, we mainly focused on AQP2. As for AQP3 and AQP4, we did not observe marked changes in their mRNA expressions. However, whether PTEN loss affected their protein level or subcellular localization and whether they contributed to impaired water balance found in *Pten*$^{\Delta/\Delta}$ mice are still unclear. Further investigations are needed to determine the exact role of AQP3 and AQP4 in *Pten*$^{\Delta/\Delta}$ mice.

AQP2 is usually localized in intracellular transport vesicles in the basal state. In the presence of external stimuli, such as dehydration or hypovolemia, arginine vasopressin is secreted and binds to V2 receptor (V2R) in the collecting ducts to activate the cAMP/PKA signaling pathway. Activated PKA then phosphorylates AQP2 at Ser256 and induces trafficking of AQP2 to the apical plasma membrane, which is critical for water reabsorption in the kidney. In this process, AQP2 phosphorylation at Ser256 is thought to be a pivotal step. Many kinases, including PKA [15–17], G-CK [19], CAMK2, AKT [20], and adenosine monophosphate kinase [52], have been reported to be involved in Ser256 phosphorylation. Among these kinases, PKA is considered the principal one. However, in the present study, the protein level of PKA C-α and phosphorylated PKA substrates slightly changed after PTEN deletion in either *Pten*$^{\Delta/\Delta}$ mice or IMCD3 cells (without significant difference, shown in online suppl. Fig. S2), suggesting that PTEN loss has a small effect on PKA activity and AQP2 phosphorylation in this study is probably attributed to other kinases.

AKT is another kinase involved in AQP2 regulation. A previous study showed that AKT activation played an important role in vasopressin-dependent AQP2 expression by increasing its mRNA level [53]. In addition, the PI3K/AKT pathway has been reported to be involved in AQP2 phosphorylation [54]. Mass spectrometry analysis further confirmed that AKT could phosphorylate AQP2 at Ser256 in vitro, suggesting that AKT activation may induce AQP2 trafficking [55]. Consistent with these previous studies, our data showed that AKT phosphorylation was upregulated and accompanied by enhanced AQP2 phosphorylation and trafficking to the apical membrane in PTEN-deficient renal collecting ducts and IMCD3 cells. Moreover, the suppression of AKT activation also reduced AQP2 phosphorylation and membrane concentration. These findings directly connected AKT activation with AQP2 phosphorylation and provided the first in vivo evidence that AKT activation played an important role in AQP2 regulation. Moreover, the underlying mechanism is still unclear. How AKT regulates AQP2 expression and phosphorylation and whether they bind to each other still need further investigation.

AKT is activated by sequential phosphorylation steps initiated by PI3K activation. After being activated by various signals, such as growth factors and G-protein-coupled receptors [56], PI3K phosphorylates the phosphatidylinositol-4,5-biphosphate to form phosphatidylinositol-3,4,5-triphosphate (PIP3) [57]. PIP3 is a lipid-derived secondary messenger that recruits phosphoinositide-dependent kinase 1 (PDK1) and AKT to the membrane through its PH domain [58, 59]. Then, the PI3K complex activates PDK1, and activated PDK1 further phosphorylates AKT at Thr308, causing a conformational change to expose the Ser473 residue [60–62]. After the conformational change, AKT can be phosphorylated at Ser473 by either autophosphorylation [63, 64] or several other kinases (PKD2 and others) to achieve its full activation [65–67]. PTEN is the most important negative regulator in this pathway. It can dephosphorylate PIP3 to phosphatidylinositol-4,5-biphosphate, thus antagonizing PI3K-induced activating signal and ultimately preventing AKT phosphorylation. PTEN loss or inactivation leads to PIP3 accumulation, which then drives AKT activation. In the present study, AKT phosphorylation at Ser473 was significantly enhanced in PTEN-deficient kidney tissues and IMCD3 cells, suggesting its full activation. To verify the important role of AKT activation in AQP2 regulation, we used two AKT inhibitors, LY and MK, to block the PI3K/AKT pathway. These two inhibitors target two steps in AKT activation. LY inhibits AKT activation by targeting PI3K and preventing PIP3 formation, which is similar to the function of PTEN, whereas MK inhibits AKT activation by directly targeting AKT and blocking its phosphorylation. Both inhibitors significantly diminished AKT phosphorylation and further attenuated AQP2 phosphorylation and membrane concentration induced by PTEN loss, confirming that AKT is an important mediator between PTEN and AQP2.

AQP2 impairment or dysregulation leads to various water balance disorders. For example, AQP2 impairment causes NDI, which is characterized by altered urine concentration and polyuria, whereas AQP2 dysregulation, including increased AQP2 expression and trafficking to the apical membrane, leads to water retention and hyponatremia in SIADH, glucocorticoid deficiency, cirrhosis, congestive heart failure, and pregnancy. In this study, PTEN loss led to AQP2 dysregulation and water retention in *Pten*$^{\Delta/\Delta}$ mice, which was similar to the aforementioned water balance disorders caused by AQP2 dysregulation.

These findings suggest that our *Pten*$^{\Delta/\Delta}$ mouse model a possible animal model for future research on these related diseases. AQP2 is pivotal for water homeostasis, which makes it a promising target for drug development of such water balance disorders. For example, Tolvaptan, a selective antagonist of V2R that can reduce AQP2 expression and membrane concentration via the arginine vasopressin/V2R/AQP2 pathway, has been applied to relieve water retention and hyponatremia in patients with heart failure, cirrhosis, and SIADH and shown promising clinical results. Sildenafil, a selective phosphodiesterase type 5 inhibitor that can activate the NO-cGMP signaling pathway and thus promote AQP2 shuttling, has been used in clinical trials of NDI, and shown a beneficial effect in decreasing urine volume and increasing urine osmolality [68]. In this study, we confirmed a new AQP2 regulation pathway, i.e., the PTEN/AKT/AQP2 pathway, which could be a possible target for further drug development. AKT inhibitors can be applied to reduce AQP2 expression and membrane concentration to relieve water retention, and PTEN inhibitors can be used to enhance AQP2 expression and membrane concentration to restore impaired urine concentration ability in NDI. However, there are also some limitations in our study. First, we did not validate the effectiveness of AKT inhibitors in the *Pten*$^{\Delta/\Delta}$ mouse model yet, which will be our future work. Second, high AKT activation should be the prerequisite for the effectiveness of AKT inhibitors, which partly limited its clinical application. Third, more studies are still needed to evaluate the efficacy and safety of these drugs, especially PTEN inhibitors, before they could be used in clinical practice.

Acknowledgments

We acknowledge the State Key Laboratory of Natural and Biomimetic Drugs from Peking University for *Ksp-Cre* mice and technical support. We thank Zhou Xiuping and Liu Xuejiao from the Institute of Nervous System Diseases of Xuzhou Medical University for their technical support. We thank Enago (www.enago.cn) for its linguistic assistance during the preparation of this manuscript.

Statement of Ethics

This study was approved by the Xuzhou Medical University Institutional Animal Care and Use Committee, approval number 201903A018. This study was performed in compliance with the ARRIVE guidelines.

Conflict of Interest Statement

The authors have no conflicts of interest to declare.

Funding Sources

This work was supported by the National Natural Science Foundation of China (Grant No. 81502387).

Author Contributions

Qingling Wang and Zhuo Sun conceived and designed the experiments. Zhuo Sun, Xiaotong Shao, and Qingling Wang drafted the manuscript. Xiaotong Shao and Zhuo Sun performed the majority of experiments, collected the data, and analyzed the results. Haotian Wu and Yaxian Zhao contributed to HE and IHC staining and assisted with Western blot analysis. Yidan Cao contributed to immunofluorescence staining. Danhua Li and Ying Sun contributed to data collection and analysis. All authors have read and approved the final version of the manuscript.

Data Availability Statement

All data generated or analyzed during this study are included in this article and its online supplementary material. Further inquiries can be directed to the corresponding author.

References

1 Guthrie D, Yucha C. Urinary concentration and dilution. Nephrol Nurs J, 2004;31(3):297–301. quiz 2–3.
2 Pearce D, Soundararajan R, Trimpert C, Kashlan OB, Deen PMT, Kohan DE. Collecting duct principal cell transport processes and their regulation. Clin J Am Soc Nephrol. 2015;10(1):135–46.
3 Lashhab R, Ullah AKMS, Cordat E. Renal collecting duct physiology and pathophysiology. Biochem Cell Biol. 2019;97(3):234–42.
4 Khositseth S, Charngkaew K, Boonkrai C, Somparn P, Uawithya P, Chomanee N, et al. Hypercalcemia induces targeted autophagic degradation of aquaporin-2 at the onset of nephrogenic diabetes insipidus. Kidney Int. 2017;91(5):1070–87.
5 Ivarsen P, Frøkiaer J, Aagaard NK, Hansen EF, Bendtsen F, Nielsen S, et al. Increased urinary excretion of aquaporin 2 in patients with liver cirrhosis. Gut. 2003;52(8):1194–9.
6 Xu DL, Martin PY, Ohara M, St John J, Pattison T, Meng X, et al. Upregulation of aquaporin-2 water channel expression in chronic heart failure rat. J Clin Invest. 1997;99(7):1500–5.
7 Nielsen S, Terris J, Andersen D, Ecelbarger C, Frokiaer J, Jonassen T, et al. Congestive heart failure in rats is associated with increased expression and targeting of aquaporin-2 water channel in collecting duct. Proc Natl Acad Sci U S A. 1997;94(10):5450–5.

8 Saito T, Saito T, Kasono K, Tamemoto H, Kawakami M, Sasaki S, et al. Hypotonicity reduces the activity of murine aquaporin-2 promoter induced by dibutyryl cAMP. Exp Physiol. 2008;93(10):1147–56.
9 Takata K, Matsuzaki T, Tajika Y, Ablimit A, Hasegawa T. Localization and trafficking of aquaporin 2 in the kidney. Histochem Cell Biol. 2008;130(2):197–209.
10 Kamsteeg EJ, Heijnen I, van Os CH, Deen PM. The subcellular localization of an aquaporin-2 tetramer depends on the stoichiometry of phosphorylated and nonphosphorylated monomers. J Cell Biol. 2000;151(4):919–30.
11 Fushimi K, Sasaki S, Marumo F. Phosphorylation of serine 256 is required for cAMP-dependent regulatory exocytosis of the aquaporin-2 water channel. J Biol Chem. 1997;272(23):14800–4.
12 Arthur J, Huang J, Nomura N, Jin WW, Li W, Cheng X, et al. Characterization of the putative phosphorylation sites of the AQP2 C terminus and their role in AQP2 trafficking in LLC-PK1 cells. Am J Physiol Renal Physiol. 2015;309(8):F673–9.
13 Katsura T, Gustafson CE, Ausiello DA, Brown D. Protein kinase A phosphorylation is involved in regulated exocytosis of aquaporin-2 in transfected LLC-PK1 cells. Am J Physiol Renal Physiol. 1997;272(6):F816–22.
14 Lu H, Sun TX, Bouley R, Blackburn K, McLaughlin M, Brown D. Inhibition of endocytosis causes phosphorylation (S256)-independent plasma membrane accumulation of AQP2. Am J Physiol Renal Physiol. 2004;286(2):F233–43.
15 Gilbert ML, Yang L, Su T, McKnight GS. Expression of a dominant negative PKA mutation in the kidney elicits a diabetes insipidus phenotype. Am J Physiol Renal Physiol. 2015;308(6):F627–38.
16 Jung HJ, Kwon TH. Molecular mechanisms regulating aquaporin-2 in kidney collecting duct. Am J Physiol Renal Physiol. 2016;311(6):F1318–28.
17 Christensen BM, Zelenina M, Aperia A, Nielsen S. Localization and regulation of PKA-phosphorylated AQP2 in response to V(2)-receptor agonist/antagonist treatment. Am J Physiol Renal Physiol. 2000;278(1):F29–42.
18 Bouley R, Breton S, Sun T, McLaughlin M, Nsumu NN, Lin HY, et al. Nitric oxide and atrial natriuretic factor stimulate cGMP-dependent membrane insertion of aquaporin 2 in renal epithelial cells. J Clin Invest. 2000;106(9):1115–26.
19 Procino G, Carmosino M, Marin O, Brunati AM, Contri A, Pinna LA, et al. Ser-256 phosphorylation dynamics of Aquaporin 2 during maturation from the ER to the vesicular compartment in renal cells. FASEB J. 2003;17(13)1886–8.
20 Douglass J, Gunaratne R, Bradford D, Saeed F, Hoffert JD, Steinbach PJ, et al. Identifying protein kinase target preferences using mass spectrometry. Am J Physiol Cell Physiol. 2012;303(7):C715–27.
21 Li J, Yen C, Liaw D, Podsypanina K, Bose S, Wang SI, et al. PTEN, a putative protein tyrosine phosphatase gene mutated in human brain, breast, and prostate cancer. Science. 1997;275(5308):1943–7.
22 Samarakoon R, Helo S, Dobberfuhl AD, Khakoo NS, Falke L, Overstreet JM, et al. Loss of tumour suppressor PTEN expression in renal injury initiates SMAD3- and p53-dependent fibrotic responses. J Pathol. 2015;236(4):421–32.
23 Fan C, Zhao C, Wang F, Li S, Wang J. Significance of PTEN mutation in cellular process, prognosis, and drug selection in clear cell renal cell carcinoma. Front Oncol. 2019;9:357.
24 Wang Y, Wang X, Wang H, Bao J, Jia N, Huang H, et al. PTEN protects kidney against acute kidney injury by alleviating apoptosis and promoting autophagy via regulating HIF1-α and mTOR through PI3K/Akt pathway. Exp Cell Res. 2021;406(1):112729.
25 Tang J, Goldschmeding R, Samarakoon R, Higgins P J. Protein phosphatase Mg2+/Mn2+ dependent-1A and PTEN deregulation in renal fibrosis: novel mechanisms and co-dependency of expression. FASEB J. 2020;34(2)2641–56.
26 Li Y, Hu Q, Li C, Liang K, Xiang Y, Hsiao H, et al. PTEN-induced partial epithelial-mesenchymal transition drives diabetic kidney disease. J Clin Invest. 2019;129(3):1129–51.
27 Shao X, Somlo S, Igarashi P. Epithelial-specific Cre/lox recombination in the developing kidney and genitourinary tract. J Am Soc Nephrol. 2002;13(7):1837–46.
28 Ophascharoensuk V, Giachelli CM, Gordon K, Hughes J, Pichler R, Brown P, et al. Obstructive uropathy in the mouse: role of osteopontin in interstitial fibrosis and apoptosis. Kidney Int. 1999;56(2):571–80.
29 Knepper M, Kwon T, Nielsen S, Molecular physiology of water balance. N Engl J Med. 2015;372(14):1349–58.
30 Pietrement C. Aquaporins in the kidney. Nephrol Ther. 2008;4(7):562–7.
31 Takata K, Matsuzaki T, Tajika Y. Aquaporins: water channel proteins of the cell membrane. Prog Histochem Cytochem. 2004;39(1):1–83.
32 Tajika Y, Matsuzaki T, Suzuki T, Aoki T, Hagiwara H, Kuwahara M, et al. Aquaporin-2 is retrieved to the apical storage compartment via early endosomes and phosphatidylinositol 3-kinase-dependent pathway. Endocrinology. 2004;145(9):4375–83.
33 Looker HC, Lin C, Nair V, Kretzler M, Mauer M, Najafian B, et al. Serum level of polyubiquitinated PTEN and loss of kidney function in American Indians with type 2 diabetes. Am J Kidney Dis. 2022;79(4):497–506.
34 Sun Z, Lu J, Wu M, Ouyang C, Xing Y, Hou X, et al. PTEN-knockdown disrupts the morphology, growth pattern and function of Nthy-Ori 3-1 cells by downregulating PAX8 expression. Oncol Lett. 2019;18(6):6732–40.
35 Du Y, Liu P, Chen Z, He Y, Zhang B, Dai G, et al. PTEN improve renal fibrosis in vitro and in vivo through inhibiting FAK/AKT signaling pathway. J Cell Biochem. 2019;120(10):17887–97.
36 Knafo S, Sánchez-Puelles C, Palomer E, Delgado I, Draffin JE, Mingo J, et al. PTEN recruitment controls synaptic and cognitive function in Alzheimer's models. Nat Neurosci. 2016;19(3):443–53.
37 Peyrou M, Bourgoin L, Poher AL, Altirriba J, Maeder C, Caillon A, et al. Hepatic PTEN deficiency improves muscle insulin sensitivity and decreases adiposity in mice. J Hepatol. 2015;62(2):421–9.
38 Horie Y, Suzuki A, Kataoka E, Sasaki T, Hamada K, Sasaki J, et al. Hepatocyte-specific Pten deficiency results in steatohepatitis and hepatocellular carcinomas. J Clin Invest. 2004;113(12):1774–83.
39 Flodby P, Liebler JM, Sunohara M, Castillo DR, McConnell AM, Krishnaveni MS, et al. Region-specific role for Pten in maintenance of epithelial phenotype and integrity. Am J Physiol Lung Cell Mol Physiol. 2017;312(1):L131–42.
40 Xing Y, Wang R, Li C, Minoo P. PTEN regulates lung endodermal morphogenesis through MEK/ERK pathway. Dev Biol. 2015;408(1):56–65.
41 Lin J, Shi Y, Peng H, Shen X, Thomas S, Wang Y, et al. Loss of PTEN promotes podocyte cytoskeletal rearrangement, aggravating diabetic nephropathy. J Pathol. 2015;236(1):30–40.
42 Wang H, Feng Z, Xie J, Wen F, Jv M, Liang T, et al. Podocyte-specific knockin of PTEN protects kidney from hyperglycemia. Am J Physiol Renal Physiol. 2018;314(6):F1096–107.
43 Zhou J, Brugarolas J, Parada LF. Loss of Tsc1, but not Pten, in renal tubular cells causes polycystic kidney disease by activating mTO RC1. Hum Mol Genet. 2009;18(22):4428–41.
44 Chen JK, Nagai K, Chen J, Plieth D, Hino M, Xu J, et al. Phosphatidylinositol 3-kinase signaling determines kidney size. J Clin Invest. 2015;125(6):2429–44.
45 Frew IJ, Thoma CR, Georgiev S, Minola A, Hitz M, Montani M, et al. pVHL and PTEN tumour suppressor proteins cooperatively suppress kidney cyst formation. EMBO J. 2008;27(12)1747–57.
46 Dizman N, Philip EJ, Pal SK. Genomic profiling in renal cell carcinoma. Nat Rev Nephrol. 2020;16(8):435–51.
47 Ricketts CJ, De Cubas AA, Fan H, Smith CC, Lang M, Reznik E, et al. The cancer genome atlas comprehensive molecular characterization of renal cell carcinoma. Cell Rep. 2018;23(12):3698.
48 Cao Z, Yu W, Li W, Cheng F, Rao T, Yao X, et al. Oxidative damage and mitochondrial injuries are induced by various irrigation pressures in rabbit models of mild and severe hydronephrosis. PLoS One. 2015;10(6):e0127143.
49 Vukićević T, Schulz M, Faust D, Klussmann E. The trafficking of the water channel aquaporin-2 in renal principal cells-a potential target for pharmacological intervention in cardiovascular diseases. Front Pharmacol. 2016;7:23.

50 Moeller HB, Fuglsang CH, Fenton RA. Renal aquaporins and water balance disorders. Best Pract Res Clin Endocrinol Metab. 2016;30(2):277–88.
51 Matsuzaki T, Yaguchi T, Shimizu K, Kita A, Ishibashi K, Takata K. The distribution and function of aquaporins in the kidney: resolved and unresolved questions. Anat Sci Int. 2017;92(2):187–99.
52 Klein JD, Wang Y, Blount MA, Molina PA, LaRocque LM, Ruiz JA, et al. Metformin, an AMPK activator, stimulates the phosphorylation of aquaporin 2 and urea transporter A1 in inner medullary collecting ducts. Am J Physiol Renal Physiol. 2016;310(10):F1008–12.
53 Bustamante M, Hasler U, Kotova O, Chibalin AV, Mordasini D, Rousselot M, et al. Insulin potentiates AVP-induced AQP2 expression in cultured renal collecting duct principal cells. Am J Physiol Renal Physiol. 2005;288(2):F334–44.
54 Pisitkun T, Jacob V, Schleicher SM, Chou CL, Yu MJ, Knepper MA. Akt and ERK1/2 pathways are components of the vasopressin signaling network in rat native IMCD. Am J Physiol Renal Physiol. 2008;295(4):F1030–43.
55 Douglass J, Gunaratne R, Bradford D, Saeed F, Hoffert JD, Steinbach PJ, et al. Identifying protein kinase target preferences using mass spectrometry. Am J Physiol Cell Physiol. 2012;303(7):C715–27.
56 Davies MA. Regulation, role, and targeting of Akt in cancer. J Clin Oncol. 2011;29(35):4715–7.
57 Vanhaesebroeck B, Leevers SJ, Ahmadi K, Timms J, Katso R, Driscoll PC, et al. Synthesis and function of 3-phosphorylated inositol lipids. Annu Rev Biochem. 2001;70:535–602.
58 Scheid MP, Woodgett JR. PKB/AKT: functional insights from genetic models. Nat Rev Mol Cell Biol. 2001;2(10):760–8.
59 Datta SR, Brunet A, Greenberg ME. Cellular survival: a play in three Akts. Genes Dev. 1999;13(22):2905–27.
60 Alessi DR, Deak M, Casamayor A, Caudwell FB, Morrice N, Norman DG, et al. 3-Phosphoinositide-dependent protein kinase-1 (PDK1): structural and functional homology with the Drosophila DSTPK61 kinase. Curr Biol. 1997;7(10):776–89.
61 Alessi DR, Andjelkovic M, Caudwell B, Cron P, Morrice N, Cohen P, et al. Mechanism of activation of protein kinase B by insulin and IGF-1. EMBO J. 1996;15(23):6541–51.
62 Stephens L, Anderson K, Stokoe D, Erdjument-Bromage H, Painter GF, Holmes AB, et al. Protein kinase B kinases that mediate phosphatidylinositol 3, 4, 5-trisphosphate-dependent activation of protein kinase B. Science. 1998;279(5351):710–4.
63 Behn-Krappa A, Newton AC. The hydrophobic phosphorylation motif of conventional protein kinase C is regulated by autophosphorylation. Curr Biol. 1999;9(14):728–37.
64 Toker A, Newton AC. Akt/protein kinase B is regulated by autophosphorylation at the hypothetical PDK-2 site. J Biol Chem. 2000;275(12):8271–4.
65 Leslie NR, Biondi RM, Alessi DR. Phosphoinositide-regulated kinases and phosphoinositide phosphatases. Chem Rev. 2001;101(8):2365–80.
66 Sarbassov DD, Guertin DA, Ali SM, Sabatini DM. Phosphorylation and regulation of Akt/PKB by the rictor-mTOR complex. Science. 2005;307(5712):1098–101.
67 Jacinto E, Facchinetti V, Liu D, Soto N, Wei S, Jung SY, et al. SIN1/MIP1 maintains rictor-mTOR complex integrity and regulates Akt phosphorylation and substrate specificity. Cell. 2006;127(1):125–37.
68 Assadi F, Sharbaf FG. Sildenafil for the treatment of congenital nephrogenic diabetes insipidus. Am J Nephrol. 2015;42(1):65–9.